Localization of serum resistance-associated protein in *Trypanosoma brucei rhodesiense* and transgenic *Trypanosoma brucei brucei*

Jean-Mathieu Bart,[1,2]* Carlos Cordon-Obras,[1] Isabel Vidal,[1] Jennifer Reed,[3] Esperanza Perez-Pastrana,[4] Laureano Cuevas,[4] Mark C. Field,[5] Mark Carrington[3] and Miguel Navarro[1]†

[1]*Instituto de Parasitología y Biomedicina 'López-Neyra', Consejo Superior de Investigaciones Científicas, Granada, Spain.*
[2]*Centro Nacional de Medicina Tropical, Instituto de Salud Carlos III, Madrid, Spain.*
[3]*Department of Biochemistry, University of Cambridge, Cambridge, UK.*
[4]*Centro Nacional de Microbiología, Instituto de Salud Carlos III, Madrid, Spain.*
[5]*Division of Biological Chemistry and Drug Discovery, University of Dundee, Dundee, UK.*

Summary

African trypanosomes infect a broad range of mammals, but humans and some higher primates are protected by serum trypanosome lytic factors that contain apolipoprotein L1 (ApoL1). In the human-infective subspecies of *Trypanosoma brucei*, *Trypanosoma brucei rhodesiense*, a gene product derived from the variant surface glycoprotein gene family member, serum resistance-associated protein (SRA protein), protects against ApoL1-mediated lysis. Protection against trypanosome lytic factor requires the direct interaction between SRA protein and ApoL1 within the endocytic apparatus of the trypanosome, but some uncertainty remains as to the precise mechanism and location of this interaction. In order to provide more insight into the mechanism of SRA-mediated resistance to trypanosome lytic factor, we assessed the localization of SRA in *T. b. rhodesiense* EATRO3 using a novel monoclonal antibody raised against SRA together with a set of well-characterized endosomal markers. By three-dimensional deconvolved immunofluorescence single-cell analysis, combined with double-labelling immunoelectron microscopy, we found that ≈ 50% of SRA protein localized to the lysosome, with the remaining population being distributed through the endocytic pathway, but apparently absent from the flagellar pocket membrane. These data suggest that the SRA/trypanolytic factor interaction is intracellular, with the concentration within the endosomes potentially crucial for ensuring a high efficiency.

Introduction

Immune evasion for African trypanosomes has multiple components. Antigenic variation is the primary mechanism based on the monoallelic expression of the variant surface glycoproteins (VSG; Cross, 1975). Additional mechanisms assisting in defence against the host immune system include rapid capping, endocytosis and degradation of surface-bound immune complexes (Barry, 1979; Pal *et al.*, 2003; Engstler *et al.*, 2007). A third component is responsible for resistance to innate immune factors and dictates host range. In particular, this governs the ability to infect humans and a number of higher primates (Pays *et al.*, 2014).

The immune effectors responsible for host restriction are trypanolytic factor (TLF) 1 and 2, serum macromolecular complexes which contain two primate-specific proteins: haptoglobin-related protein (Hpr) and apolipoprotein L1 (ApoL1). TLF1 enters the trypanosome through binding of Hpr to the haptoglobin-haemoglobin receptor (HpHbR) and clathrin-mediated endocytosis, while ApoL1 causes trypanolysis via the transmembrane flux of chloride and the osmotic swelling of the lysosome (Vanhamme *et al.*, 2003; Perez-Morga *et al.*, 2005; Thomson and Finkelstein, 2015). Trypanosomes that infect humans have evolved mechanisms that negate TLF-mediated killing. In the West Africa subspecies *Trypanosoma brucei gambiense*, the resistance mechanism appears to involve multiple factors, including

alterations to TLF endocytosis by a polymorphism in the HpHbR lowering the affinity for ligand (Vanhollebeke *et al.*, 2008; Higgins *et al.*, 2013), expression of the *T. b. gambiense*-specific glycoprotein TgsGP and reduction of sensitivity to ApoL1 through altered cysteine protease activity (Uzureau *et al.*, 2013). In the East African form, *Trypanosoma brucei rhodesiense*, a single serum resistance-associated (SRA) gene is both necessary for resistance to TLFs and sufficient to confer resistance on otherwise sensitive *Trypanosoma brucei brucei* isolates (De Greef and Hamers, 1994; Xong *et al.*, 1998). The mechanism of resistance is a stoichiometric binding of SRA to ApoL1 that prevents ApoL1 trypanocidal action (Pays *et al.*, 2014).

To gain access to the lysosome via endocytosis, ApoL1 is trafficked through the endosomal system. Endocytosis is exclusively clathrin-mediated in trypanosomes and extremely rapid in the mammalian stages. Following the initial endocytosis event at the flagellar pocket membrane, cargo progresses through a series of endosomal subcompartments that have been defined to some degree, and which correspond broadly to early, middle and late endosomes of mammalian cells plus recycling sorting/endosomes; these are defined by the presence of the small GTPases Rab 5, 21, 28 and 7 respectively for the endocytic arm and Rab11 for the recycling pathways (Manna *et al.*, 2014).

Despite a considerable body of literature, it remains unknown where the initial interaction between SRA and ApoL1 occurs within the trypanosome endosomal system, while descriptions of the localization of SRA within the cell are not always consistent. Initial reports localized endogenous SRA to solely the lysosome by immunofluorescence (IF), using p67 as the lysosomal marker (Vanhamme *et al.*, 2003). Subsequently, a wider distribution within the endosomal system, extending from the flagellar pocket to the lysosome and including several intermediate endosomes, was reported in a cell line overexpressing a Ty epitope-tagged SRA transgene. In this study, visualization of SRA in the lysosome required the use of the lysosomal protease inhibitor FMK-024, presumably to delay degradation of the SRA protein or Ty epitope (Stephens and Hajduk, 2011). These conflicting reports have significant impact in understanding the function of SRA and in particular, the likely site(s) of interaction. Does SRA bind and inactivate TLF early in the endocytic pathway or is the encounter later, at a point close to the lysosome? These points are important as they also influence the mechanism by which TLF is prevented from accessing the lysosome; specifically, the intracellular routes that are required to simply recycle TLF from early endosomes are well established, but pathways to bring material from late or terminal endosomes back to the surface are poorly documented in trypanosomes. Here,

with high resolution three-dimensional deconvolved IF (3D-IF), the subcellular localization of the SRA protein has been investigated in cell lines over a range of expression levels that spans the endogenous expression level in *T. b. rhodesiense* and two *T. b. brucei* cell lines containing SRA transgenes.

Results and discussion

Characterization of an SRA monoclonal antibody and transgenic cell lines

The mature SRA polypeptide has ~360 residues, three potential N-linked glycosylation sites and a glycosylphosphatidylinositol anchor at the C-terminus (Vanhamme *et al.*, 2003; Oli *et al.*, 2006). SRA has structural similarity to VSG, and in particular the division into a large N-terminal and smaller C-terminal domain. The N-terminal domain, corresponding to residues 24 to 267, has been modelled using a VSG template (Campillo and Carrington, 2003). The region included in that model was expressed as a recombinant protein in *Escherichia coli* (Thomson *et al.*, 2009) and used to generate monoclonal antibodies in mice (Fig. 1A). A panel of hybridomas were screened against recombinant SRA by ELISA (data not shown) and positive clones were rescreened against recombinant SRA by Western blot (WB) and finally, whole cell lysates from *T. b. rhodesiense* and *T. b. brucei* (Fig. 1B). Two monoclonal antibodies remained at this point and the monoclonal anti-SRA (5D2) that gave the strongest reactivity by WB was selected. MAb5D2 recognized a polypeptide of ~50 kDa in lysates of *T. b. rhodesiense* grown in the presence of human serum, but did not recognize any antigens in lysates from *T. b. brucei* or *T. b. rhodesiense* cultured for an extensive period in the absence of human serum, a treatment frequently resulting in silencing of the SRA gene (De Greef and Hamers, 1994; Xong *et al.*, 1998). MAb5D2 therefore represents a defined anti-SRA reagent with high specificity.

As a member of the VSG family, SRA is predicted to share similar structures with both VSGs and the trypanosome transferrin receptor (De Greef and Hamers, 1994; Carrington and Boothroyd, 1996). Evidence from *in silico* modelling of the SRA protein suggests that there are two disulphide bonds in the N-terminal domain of SRA. The small C-terminal domain of SRA shares conserved cysteine residues with the VSG C-terminal domains (Campillo and Carrington, 2003), but, in SRA, there is an additional cysteine present in the linker between the N-terminal and C-terminal domain. Significantly, a minority of VSGs also possess a cysteine in an equivalent position which forms an interchain disulphide bond in the VSG dimer. To test if SRA is a disulphide-linked dimer,
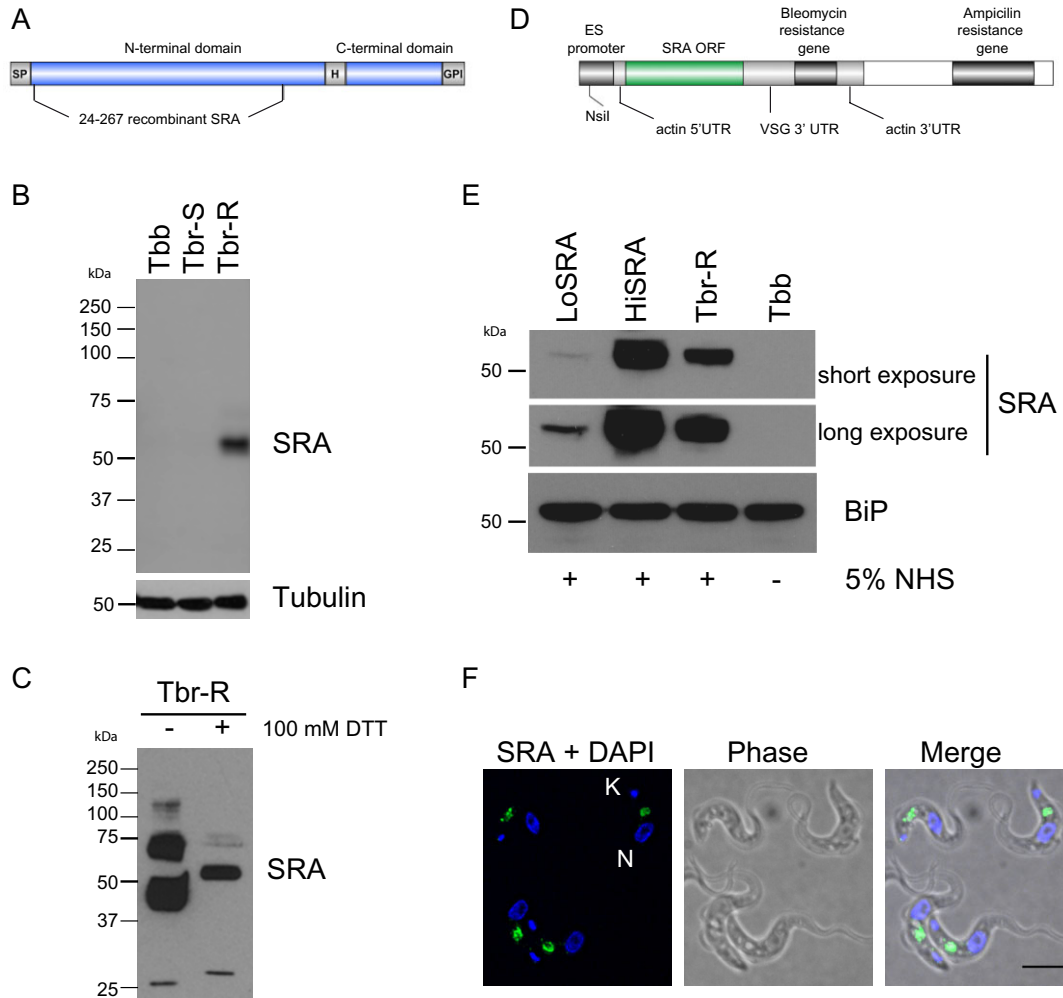
Fig. 1. Characterization of an SRA monoclonal antibody and transgenic cell lines expressing SRA.
A. Schematic representation of the recombinant SRA protein used to generate the monoclonal antibody. GPI, glycosylphosphatidylinositol anchor; HD, hinge domain; SP, signal peptide.
B. WB analysis with a mouse monoclonal antibody generated against SRA (mAb 5D2). Tubulin was used as loading control. Tbb, *Trypanosoma brucei brucei*; Tbr-S, *Trypanosoma brucei rhodesiense*-human serum sensitive; Tbr-R, *T. b. rhodesiense*-human serum resistant.
C. WB analysis with anti-SRA of *T. b. rhodesiense* protein extracts in the presence or absence of 100 mM DTT.
D. Schematic representation of the plasmid used to ectopically express SRA in *T. b. brucei*.
E. WB analysis of *T. b. brucei* cell lines ectopically expressing SRA (LoSRA and HiSRA). BiP was used as loading control. Two exposure times are shown (30 s as short exposure and 3 min as long exposure).
F. IF analysis of the endogenous SRA (green) expression pattern in *T. b. rhodesiense*. DNA is stained with DAPI. Scale bar: 5 μm.

protein extracts of normal human serum (NHS)-resistant *T. b. rhodesiense* (Tbr-R) were prepared in the absence or presence of 100 mM of DTT. After WB analysis, DTT-treated SRA protein migrated as the expected 50 kDa single band, while two major species at ~40 kDa and ~70 kDa and a minor one at 130 kDa were detected for the untreated extract (Fig. 1C). The most likely interpretation is that the 40 kDa form is the SRA monomer with disulphide bonds intact and the 70 kDa form is an SRA

dimer, suggesting that SRA is present as both disulphide-bonded dimers and non-disulphide-bonded forms within the cell. The higher molecular weight form may represent an additional oligomeric state.

To create cell lines expressing different levels of SRA protein, a transgene encoding the complete SRA open reading frame, flanked by an actin 5'UTR and VSG 3'UTR, was introduced ~400 bp downstream of the VSG promoter in an expression site (Penate *et al.*, 2009;

Fig. 1D). Cell lines containing the transgene were screened by WB with the monoclonal anti-SRA and two cell lines were selected for experiments, with one expressing significantly less SRA (LoSRA) than *T. b. rhodesiense* and one expressing more SRA (HiSRA; Fig. 1E).

To confirm the correct folding of SRA and its ability to confer resistance to NHS, both clones were grown in 5% fresh and inactivated NHS, together with the *T. b. brucei* S16 parental cell line. While S16 cells died within 24 h in such conditions, the two transgenic SRA clones proliferated indistinguishably from *T. b. rhodesiense* (data not shown) validating that the transgenic SRA was both folding and being targeted correctly.

To localize SRA in *T. b. rhodesiense* cells, we carried out 3D-IF microscopy on cells grown in the presence of 5% human serum. Statistical analysis of the SRA distribution was performed using interphase cells (i.e. 1K1N) and specifically excluding cells undergoing mitosis or cytokinesis where SRA localization is significantly more complex, most likely due to the replication and segregation of cellular organelles. Consistent with earlier studies, SRA demonstrated significant distribution to regions of the cell between the nucleus and kinetoplast, which is consistent with a location throughout the endocytic pathway (Fig. 1F). Significantly, we were unable to detect SRA at the surface of the parasite or in a region close to the kinetoplast, where the flagellar pocket resides, suggesting that the majority of the SRA we were able to visualize was present within internal cellular structures. For 70.5% of the cells ($n = 156$), SRA concentrates in one or two areas more proximal to the nucleus than kinetoplast (see quantitation in Fig. 4B). Under our fixation and permeabilization conditions [2% paraformaldehyde (PFA) w/v and 1% NP40 v/v], SRA immunoreactivity was found close to the flagellar pocket only in a very small proportion of the cells (3.2%).

Endogenous SRA is partially associated with the lysosome in T. b. rhodesiense

Because the subcellular localization of SRA has not been definitively described in the literature (Vanhamme *et al.*, 2003; Stephens and Hajduk, 2011), we re-examined SRA localization taking advantage of MAb5D2 and combined this with high resolution 3D-deconvolution imaging (Landeira *et al.*, 2009) performed in *T. b. rhodesiense*. To determine the proportion of colocalization between SRA and the lysosome, two independent lysosomal markers were used: p67 and TbCathepsin (TbCatL), a lysosomal protease, also known as trypanopain (Caffrey *et al.*, 2001; Fig. 2A). Single-cell quantification was performed from the 3D-deconvolved images using JACoP, a component of ImageJ. Under permeabilizing conditions,

SRA partially localized with both lysosomal markers; Pearson's coefficients were statistically significant when comparing SRA/TbCatL (rp = 0.69 ± 0.07) and SRA/p67 (rp = 0.50 ± 0.11) with the Pearson's coefficient calculated to examine the colocalization between SRA and BiP and endoplasmic reticulum (ER) marker (rp = 0.33 ± 0.08; Fig. 2B). As a marker of recycling endosomes we used an antibody to TbRab11 and double IF was carried out with anti-SRA MAb5D2 (Fig. 2A, lower panel). No colocalization was found between both proteins (rp = 0.19 ± 0.13), discarding the possibility of a significant presence for SRA in the exocytic or recycling pathways. Finally, to assess a possible location of SRA in the flagellar pocket area as previously suggested (Stephens and Hajduk, 2011), we combined anti-SRA with a rabbit polyclonal anti-FTZC antibody that was described as a component of the flagellum transition zone, located at the base of the flagellum (Bringaud *et al.*, 2000). Double IF followed by single-cell analysis failed to detect any significant colocalization between SRA and FTZC (rp = 0.08 ± 0.04; Fig. 2A and B), suggesting that in endogenous conditions, SRA does not traffic through flagellar pocket area.

For both lysosomal markers that showed significant colocalization, we decided to apply Mander's M1 and M2 coefficients that quantitate the portion of the intensity in each channel that coincides with some intensity in the other channel. These data represent the ratio of intersecting volumes, but considering each channel separately. For cells stained with TbCatL and SRA, 49.5% (±16.1%) of the signal detected for TbCatL (M1) coincided with SRA signal, while 67.6% (±16.3%) of SRA (M2) coincided with TbCatL (Fig. 2C). Congruently with the Pearson's coefficient data calculated for p67 and SRA, Mander's coefficients decreased in comparison with the TbCatL/SRA relation with 39.9% (±15.2%) of p67 signal (M1) that coincided with SRA and 36.8% (±18.1%) of SRA signal (M2) coinciding with p67. These results strongly support that SRA traffics to the lysosome, as approximately half of the SRA is detected in this compartment.

To confirm the SRA subcellular distribution analysed by 3D-IF, we decided to conduct immunoelectron microscopy (IEM) combining anti-p67 (lysosome) and anti-FTZC with the monoclonal anti-SRA antibody. To guarantee relevant IEM labelling conditions, antibodies were first studied separately. As expected, both rabbit polyclonal antibodies gave a characteristic pattern shown in Fig. 3A for anti-p67 and in Fig. 3B and C for anti-FTZC. Despite the low sensitivity of the antibody, a specific anti-SRA MAb5D2 signal was observed; 15 nm gold particles were associated with vesicles as revealed in Fig. 3D. We thus decided to perform double IEM, combining anti-SRA either with anti-p67 or anti-FTZC.
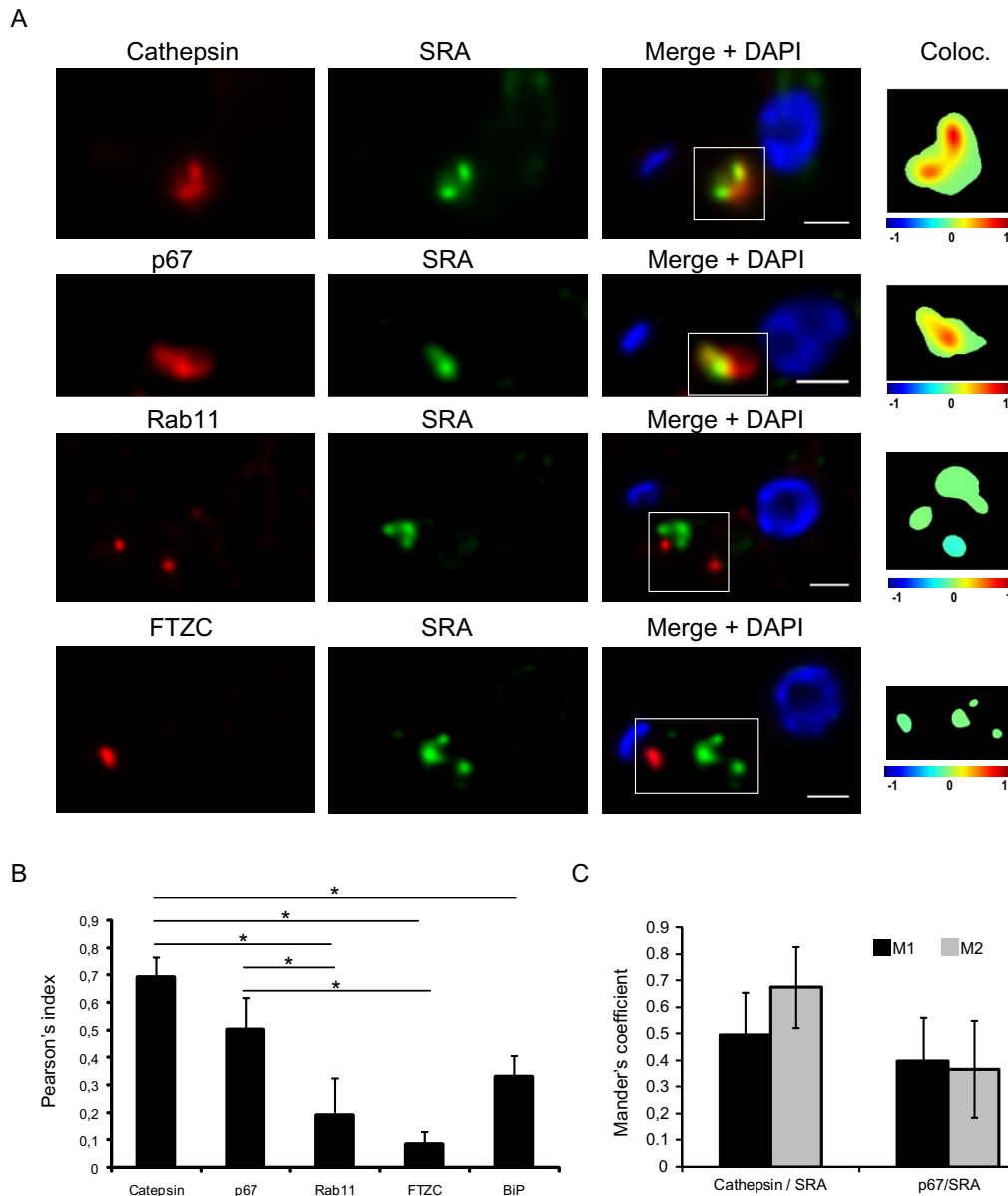
Fig. 2. SRA partially associates with lysosome.
A. Representative pictures of double 3D-IF combining rabbit polyclonal anti-cathepsin, anti-p67, anti-Rab11 or anti-FTZC antibodies (red) with the mouse monoclonal anti-SRA (5D2) antibody (green). The colocalization colour map (inset) shows the intensity of colocalization between SRA and the red-labelled endocytic markers as indicated by the colour bar. In these colour maps, the −1 to +1 heat map depicts the measured icorr values. Negatively correlated relationships (icorr values between −1 and 0) are shown in blue-green colours, whereas positive correlations (icorr values between 0 and 1) are represented by warmer yellow-red colours. Scale bar: 1 μm.
B and C. Colocalization analysis. Pearson's coefficient was calculated for each individual 3D-deconvolved image ($n = 70$). *P-value < 0.05.
Mander's coefficients were calculated (when Pearson's coefficient ≥ 0.5) to define the M1 and M2 as the percentages of pixels in one channel (M1 = red) that intersect with some signal in other channel (M2 = green). Both coefficients were assessed using 'JACoP', a colocalization plug-in available in Image J.

We first ensured the lack of cross-reaction between the first and the second antibodies (data not shown) and then performed double IEM. Congruently with the 3D-IF observations, SRA was never found associated with FTZC or the flagellar pocket area (Fig. 3E) while partial colocalization of SRA/p67 was confirmed (Fig. 3F). From all these data, we can also hypothesize that the remaining SRA signal that does not associate with the lysosome vesicles could be connected with the endosomal structures.
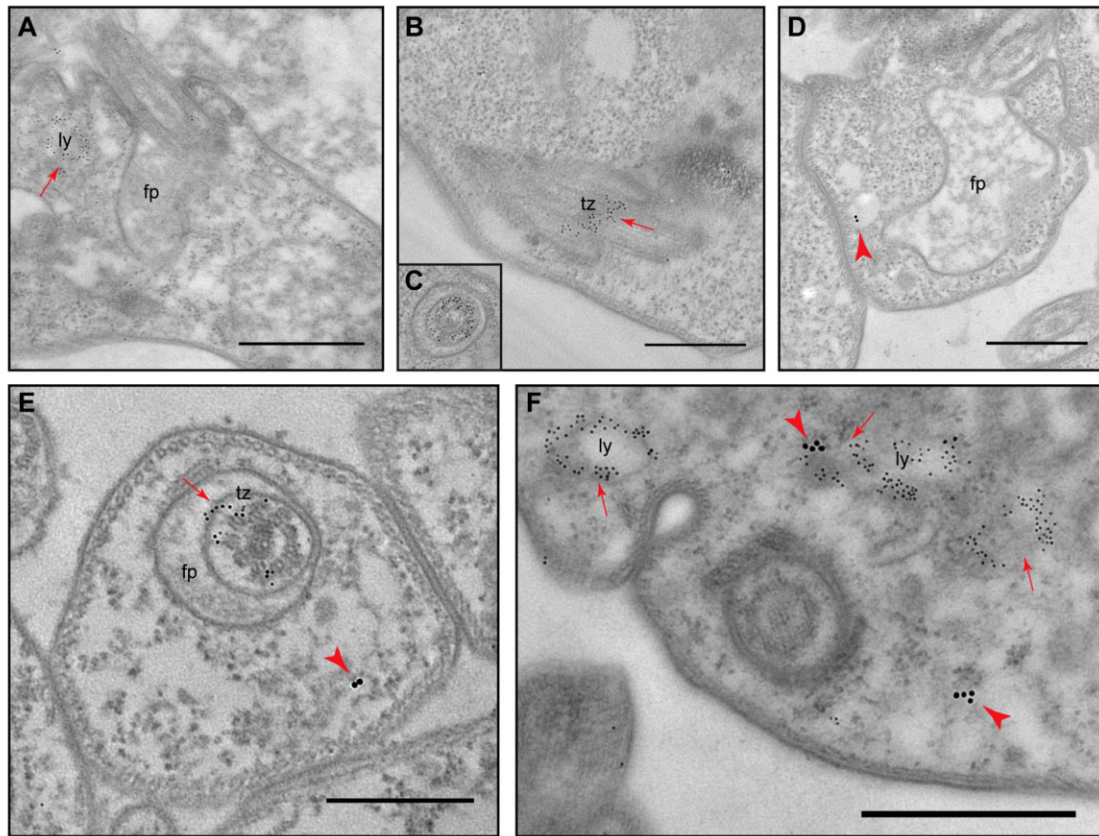
Fig. 3. Colocalization of SRA to the vicinity of lysosomes in *Trypanosoma brucei rhodesiense* NHS-resistant cell line by double-labelling IEM. Cells were first labelled either with rabbit anti-p67 (A) or rabbit anti-FTZC (B and C) or mouse anti-SRA (D) antibodies. Double-labelling was then performed with anti-SRA/anti-FTZC (E) and anti-SRA/anti-p67 (F). Arrowheads indicate SRA labelling (15 nm gold particles conjugated) and arrows indicate p67 or FTZC labelling (5 nm gold particles conjugated). fp, flagellar pocket; ly, lysosome; tz, transition zone. Scale bar: 1 μm.

Overexpression of SRA affects subcellular localization

To determine if the location of SRA is influenced by copy number, we conducted SRA IF on our transgenic *T. b. brucei* cells that are under- or overexpressing SRA (Fig. 4). As for endogenous expression in *T. b. rhodesiense*, statistical analysis was performed of the SRA distribution in 1K1N cells (Fig. 4A for IF and Fig. 4B for statistical data). For the LoSRA line, the localization of SRA was comparable with that obtained from *T. b. rhodesiense*, with ~70% to 80% of the cells exhibiting SRA as one or two punctae suggesting restriction to the lysosome and endosomes. No association was observed with the ER, as revealed by a rabbit polyclonal anti-BiP antibody (Fig. 4A). For the HiSRA cell line, we found that SRA localization was significantly more extensive, with 36.9% (±3.8%) of the cells displaying a localization that was distinct to *T. b. rhodesiense*, while 32.6% (±2.4%) of cells exhibited SRA in the flagellar pocket area. Additionally, for these cells, colocalization with BiP was observed, suggesting that when overexpressed SRA is not efficiently

folded or exported and remains within the ER and possibly Golgi apparatus (Fig. 4A).

Inhibition of endocytosis does not affect the endogenous SRA location in T. b. rhodesiense

In order to better assess the possibility that SRA traffics into the flagellar pocket, despite having an undetectable presence at steady state, we used two approaches to disrupt endocytosis. We reasoned that if even small levels of SRA were present within the flagellar pocket, the blockade to endocytic trafficking would result in accumulation of SRA at that site and facilitate the detection of SRA that was essentially *en route* via the surface.

Firstly, we monitored the location of fluorescein isothiocyanate (FITC)-labelled lectin Concanavalin A (Con A) and 488-labelled human transferrin (HT-488) in mid-log phase bloodstream form (BSF) *T. b. rhodesiense* at 4, 14 and 37 C. Both reagents report on endocytosis of surface protein; Con A by binding oligomannose N-glycans
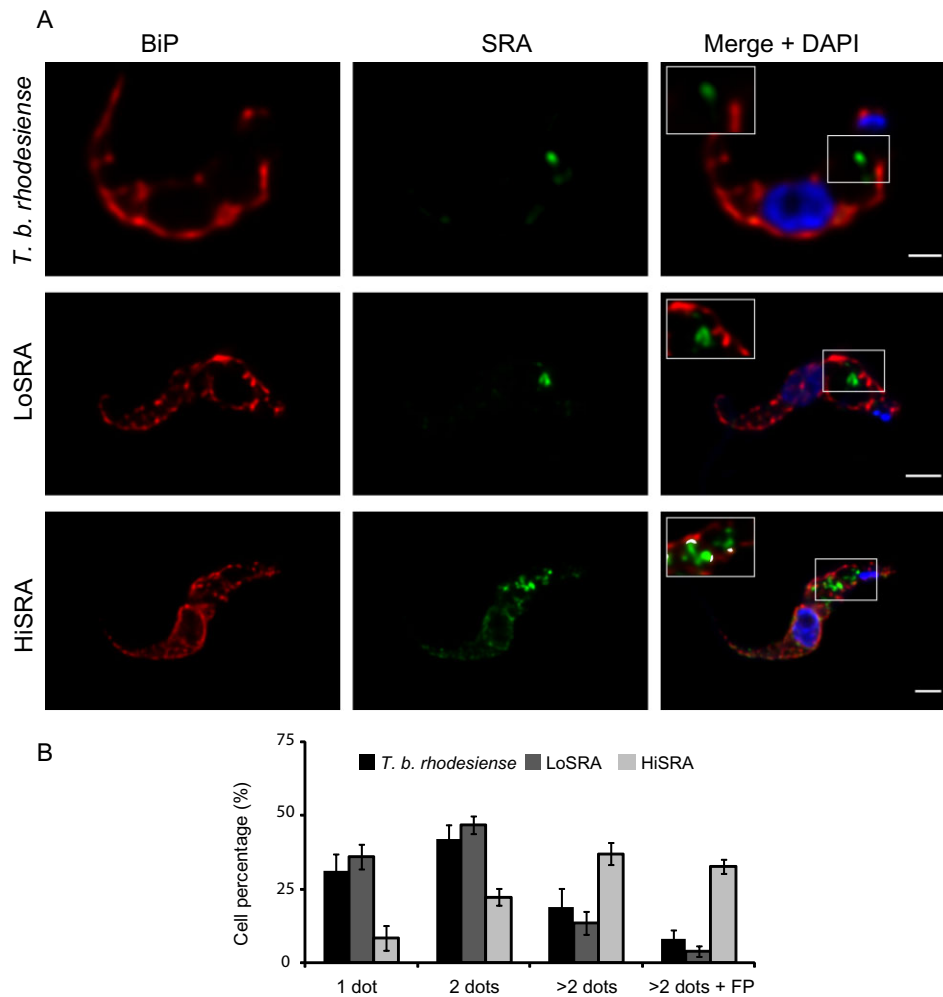
Fig. 4. Overexpression of SRA affects its subcellular localization.
A. Double indirect 3D-IF was performed in bloodstream *Trypanosoma brucei* (*Trypanosoma brucei rhodesiense*, *Trypanosoma brucei brucei* LoSRA and *T. b. brucei* HiSRA) with anti-BiP (red), anti-SRA mAb (green) and DAPI staining (blue). Higher magnification is shown in the inset, showing anti-SRA and anti-BiP fluorescence signals colocalization mask (white). Scale bars: 1 μm.
B. Statistical analysis from the SRA pattern observed by 3D-IF depending on the presence of one, two or more than two dots and its localization in the flagellar pocket area (carried out from three independent experiments, $n = 572$).

(essentially VSG) and transferrin by binding the ESAG6/7 transferrin receptor. Con A and HT-488 labelling was followed by immunostaining with anti-FTZC (Bringaud *et al.*, 2000) after fixation and permeabilization (Fig. 5A). For both reagents, low temperature clearly led to a decrease in endocytosis as expected. At 4°C, Con A and HT-488 were retained at the flagellar pocket, as colocalization with FTZC proved. This association was progressively lost when temperature increased. At 14°C, Con A and HT-488 are internalized to the endocytic system and at 37°C, both compounds reached the lysosome (Fig. 5A). We thus decided to use such conditions to assess the subcellular location of SRA upon endocytic perturbation (Fig. 5C and D). Significantly, the localization of SRA was unaltered by these low temperature treatments, retaining indistinguish-

able distributions to our previous physiological conditions. While no evidence of SRA enrichment in the flagellar pocket area was detected, colocalization of SRA with Con A and HT was significant when these fluorophores were endocytosed and trafficked through endosomes to the lysosome (see statistics in Fig. 5B).

Low temperature is not only a specific endocytic pathway inhibition, but also perturbs exocytosis and many other cellular processes (Yeaman *et al.*, 2001). Exocytosis to the cell surface is via the flagellar pocket (Grunfelder *et al.*, 2003; Sutterwala *et al.*, 2007) and alterations to exocytosis could modulate the inhibition of endocytosis and mask a putative enrichment of SRA in the flagellar pocket. Therefore, to inhibit endocytosis in a very distinct manner, we suppressed expression of
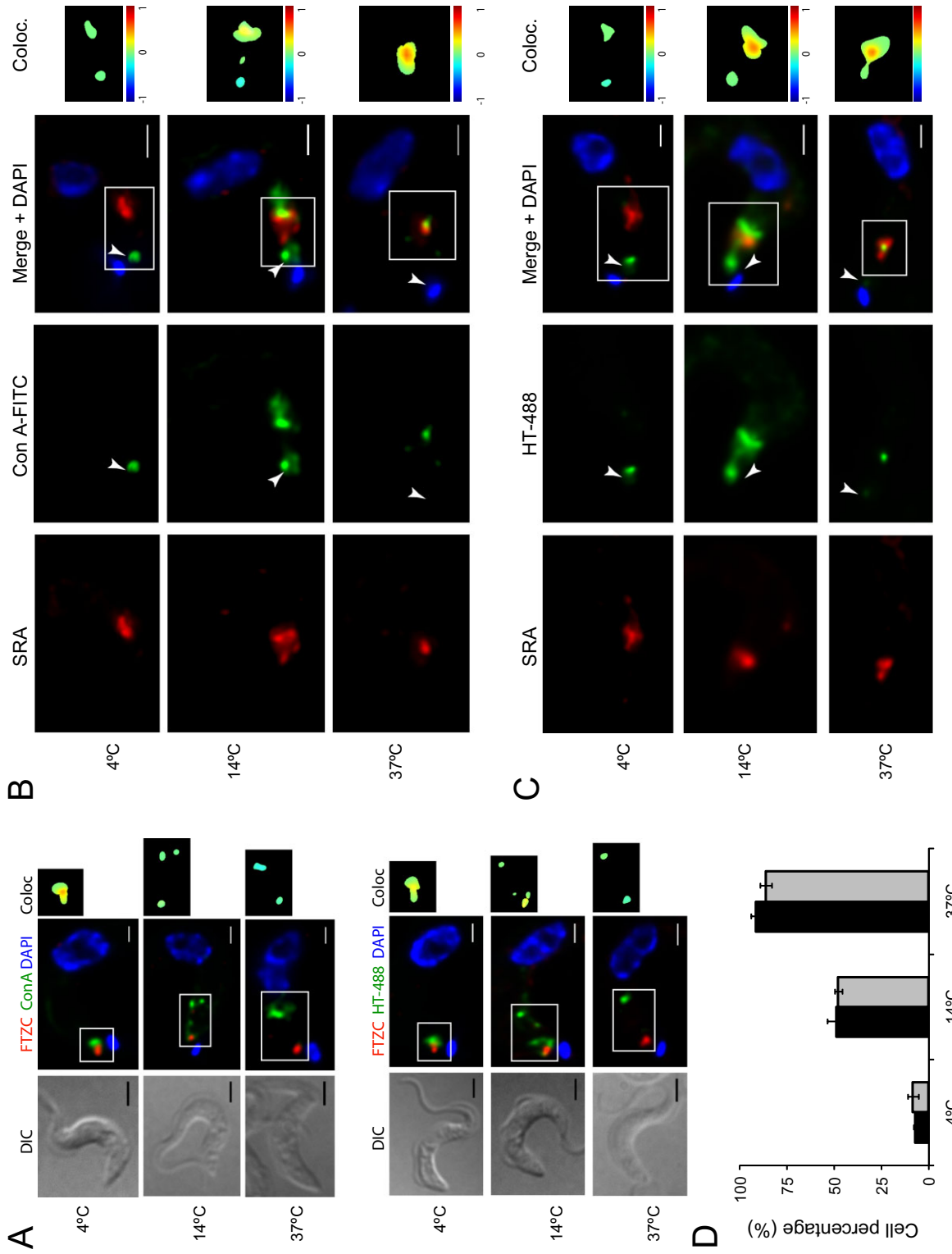
Fig. 5. Inhibition of endocytosis pathway induced by low temperature does not affect endogenous SRA localization in *Trypanosoma brucei rhodesiense.*
A. To set up the temperature-mediated endocytic inhibition, Con A-FITC and HT-488 (green) uptake was combined with 3D-IF with anti-FTZC antibody (red) upon three different temperatures (4, 14 and 37°C). At 4°C, both reagents are retained at the flagellar pocket and associate with FTZC. At 14°C, Con A and HT-488 are internalized to the endocytic system. At 37°C, both compounds are delivered to the terminal lysosome and do not associate anymore with FTZC.
B. Con A-FITC (green) uptake was combined with 3D-IF with anti-SRA antibody (red). After fixation, cells were subjected to IF with the mouse monoclonal anti-SRA antibody (red). Arrowheads indicate flagellar pocket area.
C. HT-488 (green) uptake combined with 3D-IF with anti-SRA antibody (red). The same protocol was applied as in B. Scale bars were 2 μm for differential interference contrast (DIC) and 1 μm for IF.
D. Statistical analysis of the colocalization of SRA with Con A-FITC or HT-488 depending on the temperatures (4, 14 or 37°C) calculated from two independent experiments for each reagent (n = 500).

the clathrin heavy chain (TbCLH) by RNA interference (RNAi). Knockdown (KD) of clathrin results in an enlargement of the flagellar pocket, suggesting that membrane delivery is unaffected but removal is blocked (Allen *et al.*, 2003). As *T. b. rhodesiense* EATRO3 does not contain the relevant transgenic elements for RNAi, we decided to take advantage of the *T. b. brucei* cell line expressing SRA (LoSRA).

We first monitored TbCLH depletion by measuring the uptake of Alexa-488 (HT-488) HT by flow cytometry. After only 8 h of RNAi induction, HT-488 uptake was reduced by 58.2% (±5.1%; Fig. 6A). To confirm this, fluorescence microscopy was also used. Statistical analysis performed on a total of 372 cells, analysed in two independent experiments, showed that under normal conditions, for 90.1% (±1.8%) of the cells, HT was localized in the endosomes/lysosome area after 10 min of uptake (Fig. 6B). Consistent with the flow cytometry, under TbCLH-KD, 75.4% (±2.7%) of the cells retain HT in the flagellar pocket area, while the remaining cells did not show any labelling (Fig. 6B).

Single-cell analysis ($n = 88$) of 3D-deconvolved pictures was performed using a colocalization colour map to ascertain the impact on SRA. Rapid transferrin uptake in the parental cell line leads to partial colocalization between the HT-488 and SRA in the endosomes/lysosome area (98% of the cells, Fig. 6C). For the TbCLH-induced RNAi line (LoSRA-TbCLH-KD), SRA was not significantly associated with HT. A colocalization mask indicated 11.5% of the cells with overlapping between HT-488 and SRA (with a non-significant P-value = 0.111 with Fisher's exact test), suggesting than upon such condition of strong endocytic inhibition, SRA did not significantly enrich in the flagellar pocket area (Fig. 6C and D), suggesting that SRA does not commonly traffic there.

SRA represents a key protein that confers full human serum resistance when expressed in *Trypanosoma brucei* and its intracellular itinerary is crucial to understanding the function, as the location of SRA determines where it interacts with TLF. Previous work on SRA subcellular localization lead to contradictory data (Vanhamme *et al.*, 2003; Stephens and Hajduk, 2011). Here, we attempt, using a new reagent combined with modulation of expression and trafficking, to determine specifically if SRA is either at the surface, in the flagellar pocket area or in the endocytic pathway. In summary, our data suggest that SRA is present at the internal membranes, but that even with an endocytosis block, its detection at the cell surface is not significant, suggesting that the flagellar pocket does not represent a major site for interaction between SRA and TLF (Fig. 7). The concentration of SRA within endosomes may act as a mechanism to increase the local concentration and therefore ensure efficient sequestration of TLF.

Experimental procedures

Ethics statement

Human blood samples were taken from healthy donors, who provided written informed consent for the collection of samples. These samples were specifically obtained for this study. The procedure was approved by the ethical committee of the Institute of Parasitology and Biomedicine Lopez-Neyra (Spanish National Research Council).

Trypanosomes

Trypanosoma brucei rhodesiense East African Trypanosomiasis Research Organization (EATRO3 ETat1.2 TREU164; Turner *et al.*, 2004) and *T. b. brucei* single marker [derived from *T. brucei* bloodstream, Molteno Institute Trypanozoon antigenic type (MITat) 1.2; clone 221a] cell lines (Wirtz *et al.*, 1999), grown in Hirumi's Modified Iscove (HMI)-9 medium supplemented with 10% inactivated fetal calf serum (Hirumi and Hirumi, 1989) or 5% inactivated NHS, were used for all the experimental procedures.

Production of the monoclonal antibody raised against SRA

His-tagged recombinant SRA (residues 24 to 267) was expressed in *E. coli* from plasmid p3303, a pET15b derivative (Thomson *et al.*, 2009). The polypeptide was purified using nickel ion affinity chromatography under standard conditions. A BALB/c mouse was immunized by three intraperitoneal injections of 50 μg of purified recombinant SRA. Three days before fusion, 40 μg of the protein was injected intravenously. Normal antibody-producing spleen cells were fused with immortal myeloma cells. The hybridoma that produced the desired antibody was selected by ELISA and subcloned to obtain a single epitope antibody, which was named 5D2. This monoclonal antibody was tested by WB and IF against Tbr-R, NHS-sensitive *T. b. rhodesiense* (Tbr-S) and *T. b. brucei* cell lines.

SRA expressing trypanosome

The SRA open reading frame was cloned by PCR using oligonucleotides 5′GGATCCATGCCCCGAAATTCGGGCCG-3′ and 5′-GGATCCTTAAAACAGAAAGGCCACAA-3′, digested with BamHI (underlined nucleotides) and cloned into an expression vector (pMig104) designed to integrate 405 bp downstream of the active Expression Site (ES) promoter (Penate *et al.*, 2009). Correct orientation was confirmed by sequencing. The 221-VSG 3′UTR was cloned by PCR using oligonucleotides 5′-ATGGATCCACCCCTCTTTGGCTTGCAGTT-3′ and 5′-CTCGGGCCCGTCCAGGATAGAGGTGTGAGTTAAA-3′, digested with BamHI and SmaI, respectively, and inserted downstream of the SRA Open Reading Frame (ORF) stop codon. *T. b. brucei* bloodstream-formed single marker trypanosomes were transfected and selected with 5 μg ml⁻¹ bleomycin using procedures previously described (Wirtz *et al.*, 1999). Transformants were called LoSRA and HiSRA.

RNAi procedure

To generate clathrin-depleted cell lines, the plasmid p2T7TiCLH was transfected into the LoSRA (Allen *et al.*, 2003).
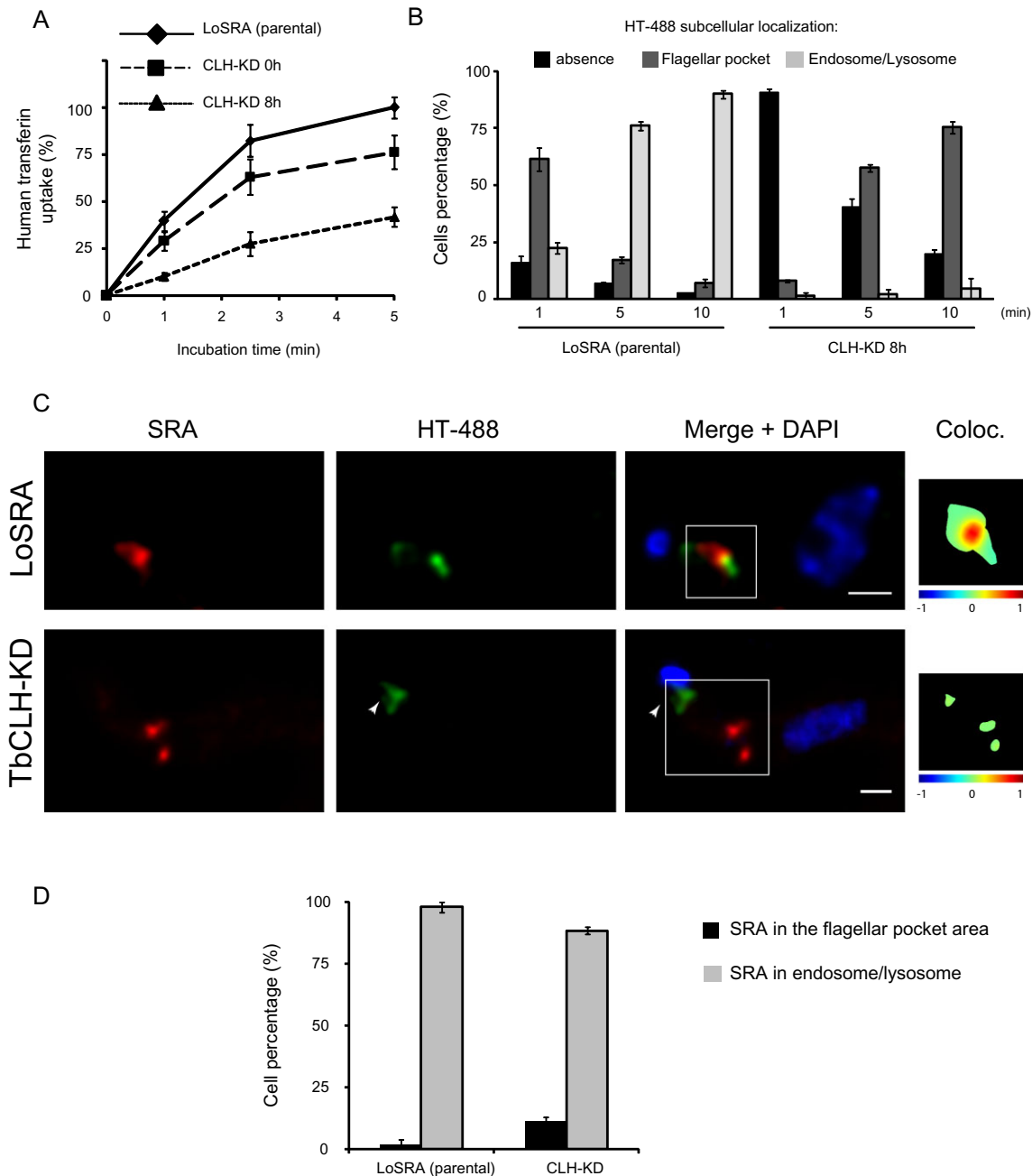
Fig. 6. Inhibition of endocytosis pathway by TbCLH-KD does not affect SRA localization.
A. HT-488 uptake analysis by flow cytometry, upon KD of TbCLH.
B. Statistical analysis of the HT-488 subcellular localization upon KD of TbCLH after 1, 5 or 10 min of HT incubation.
C. Representative IF pictures combining HT-488 (green) 5-min uptake with SRA (red) immunostaining with the 5D2 monoclonal antibody. Upper panel: parental cell line. Lower panel: TbCLH-KD. The colocalization colour map (inset) shows the intensity of colocalization between SRA and HT-488 as indicated by the colour bar. Arrowheads indicate flagellar pocket area. Scale bars, 1 μm.
D. Statistical analysis of the presence or absence of SRA in the flagellar pocket area upon TbCLH-KD ($n = 88$). No statistical significance (P-value $= 0.111$) was observed.

Transformants were selected with 2.5 μg ml^{-1} of G418, 5 μg ml^{-1} of hygromycin and 5 μg ml^{-1} of bleomycin. Clones were induced with tetracycline and selected for growth defect and transferrin uptake decrease (see *Uptake assays*).

Protein electrophoresis and WB

For protein extraction, mid-log phase cells were harvested, washed in TDB-glucose and resuspended in SDS-
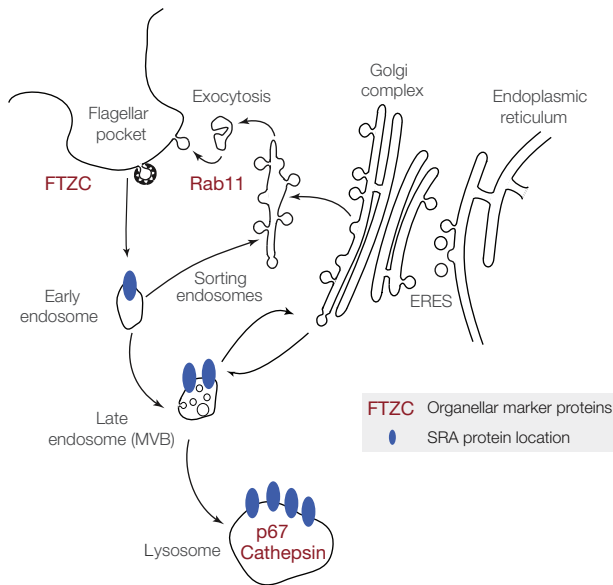
Fig. 7. Schematic model of SRA subcellular localization in *Trypanosoma brucei rhodesiense*, inferred from the data obtained with the mouse monoclonal anti-SRA antibody. Double IFs and IEMs, combining anti-SRA with various endocytic pathway markers, through endogenous conditions and/or compromising physically or molecularly the endocytosis, indicate that SRA traffics from lysosomes to endosomes, avoiding the flagellar pocket area. Our data suggest that the SRA interacts with the trypanolytic factor in an intracellular manner, with the concentration within the endosomes potentially crucial for increasing efficiency.

polyacrylamide sample buffer at a concentration of 1×10^6 cell equivalents per microlitre. Samples were electrophoresed on 10% SDS-PAGE gels at 5×10^6 cell equivalents per lane and then transferred to Hybond-ECL nitrocellulose membrane (Amersham Pharmacia Biotech). Transfer and equivalence of loading were checked by staining the membrane with Ponceau S solution (Sigma) prior to blocking for 20 min at room temperature in blocking solution (PBS supplemented by 5% dried milk). Membranes were incubated for 1 h at room temperature with primary antibody at the appropriate dilution in 0.5% blocking solution (mouse monoclonal anti-TbSRA antibody was diluted 1:10, the mouse monoclonal anti-tubulin 1:5000 and the rabbit anti-Bip 1:20 000), washed 3×10 min in PBS/0.05% Tween-20, then incubated for 1 h with horseradish peroxidase goat anti-mouse conjugate (GE Healthcare). After washing, bound antibodies were detected by reaction with luminol and visualized by exposure to X-ray film.

Uptake assays

For colocalization studies of SRA with FITC-labelled Con A (Vector Laboratories) and human holo-Tf Alexa Fluor 488-conjugated (HT-488) (Invitrogen), uptake assays were performed as followed. A total of 2×10^6 parasites, previously washed with TDB-glucose plus 1% BSA and cooled down for 10 min at 4°C, were incubated with 10 µg FITC-Con A or 5 µg HT-488 at the appropriate temperatures (4, 14 and 37°C) for 30 min in a volume of 250 µl. After incubation, cells were fixed for 1 h at 4°C in 1%

PFA diluted in cold TDB. Cells were finally washed twice with TDB to remove unlabelled Con A or HT-488 and PFA and were kept at 4°C before IF.

For analysis of HT uptake by flow cytometry, 2×10^6 trypanosomes were harvested and washed with TDB-glucose plus 1% BSA, resuspended in 250 µl in the same buffer and incubated for 10 min at 37°C. Then, 5 µg of HT-488 were added. Incubations were carried out for 0 (no Tf), 1, 2.5, 5 and 10 min at 37°C. Cells were then fixed at least for 1 h at 4°C in 1% PFA diluted in cold PBS. Parasites were finally washed twice with PBS and labelled cells were analysed with a Becton Dickinson FACSCalibur™ flow cytometer (BD Biosciences) using BD CellQuest™ Pro version 4.0.2 software (Cordon-Obras *et al.*, 2013).

3D-IF

Cellular localization analysis was performed by 3D-IF as described previously (Landeira *et al.*, 2009). Images displayed in the figures are maximum intensity projections from digitally deconvolved multichannel 3D image datasets using Huygens Essential software v. 2.9 (Scientific Volume Imaging). Cells were fixed with 2% PFA for 1 h and permeabilized with 1% NP40 for 30 min. IF analysis was carried out in 0.5% blocking reagent (Roche) in PBS (Sigma) using the mouse monoclonal anti-TbSRA antibody (5D2) (1:50), the rabbit polyclonal anti-BiP (1:20000), anti-p67 (1:4000), anti-TbCat (1:4000), anti-Rab11 (1:250) and anti-FTZC (1:2000) antibodies. Pseudocolouring and maximum intensity projections were performed using ImageJ software v. 1.43 (National Institutes of Health). Deconvolution of 3D images was performed using Huygens Essential software (version 2.9; Scientific Volume Imaging) using an experimentally calculated point-spread function with 0.2-µm TetraSpeck microspheres (Invitrogen). For the colocalization analysis, JACoP and Colocalization Colormap, available under Image J, were used. Live-cell imaging was performed at 37°C and cells were visualized under differential interference contrast optics.

IEM

Parasites were washed in TDB-glucose and fixed in 4% PFA and 0.25% glutaraldehyde in PBS, pH 7.4, 1 h at 4°C. The cell pellet was embedded in LRWhite resin (Electron Microscopy Science) and polymerized at −20°C with ultraviolet light. Thin sections (50–70 nm) were cut and probed with anti-SRA (1:2), anti-p67 (1:4000) and/or anti-FTZC (1:2000) antibodies diluted PBS with 1% BSA, 0.5% Tween 20 (Sigma), 2 h at room temperature. Primary antibody incubation was followed by 1:30 dilution goat anti-mouse (15 nm) and/or anti-rabbit (5 nm) gold conjugated antibodies (British Biocell International) incubation for 1 h. Control preparations processed without primary antibody and irrelevant primary antibodies were all negative.

Statistical analysis

We used one-way analysis of variance to compare the Pearson's coefficient value generated by the JACoP analysis. Confidence intervals were set at 95%. IBM SPSS Statistics software (version 20) was used to perform the statistical analysis.

References

Allen, C.L., Goulding, D., and Field, M.C. (2003) Clathrin-mediated endocytosis is essential in Trypanosoma brucei. *EMBO J* **22:** 4991–5002.

Barry, J.D. (1979) Capping of variable antigen on *Trypanosoma brucei*, and its immunological and biological significance. *J Cell Sci* **37:** 287–302.

Bringaud, F., Robinson, D.R., Barradeau, S., Biteau, N., Baltz, D., and Baltz, T. (2000) Characterization and disruption of a new *Trypanosoma brucei* repetitive flagellum protein, using double-stranded RNA inhibition. *Mol Biochem Parasitol* **111:** 283–297.

Caffrey, C.R., Hansell, E., Lucas, K.D., Brinen, L.S., Alvarez Hernandez, A., Cheng, J., *et al.* (2001) Active site mapping, biochemical properties and subcellular localization of rhodesain, the major cysteine protease of *Trypanosoma brucei rhodesiense*. *Mol Biochem Parasitol* **118:** 61–73.

Campillo, N., and Carrington, M. (2003) The origin of the serum resistance associated (SRA) gene and a model of the structure of the SRA polypeptide from *Trypanosoma brucei rhodesiense*. *Mol Biochem Parasitol* **127:** 79–84.

Carrington, M., and Boothroyd, J. (1996) Implications of conserved structural motifs in disparate trypanosome surface proteins. *Mol Biochem Parasitol* **81:** 119–126.

Cordon-Obras, C., Cano, J., Gonzalez-Pacanowska, D., Benito, A., Navarro, M., and Bart, J.M. (2013) *Trypanosoma brucei gambiense* adaptation to different mammalian sera is associated with VSG expression site plasticity. *PLoS ONE* **8:** e85072.

Cross, G.A. (1975) Identification, purification and properties of clone-specific glycoprotein antigens constituting the surface coat of *Trypanosoma brucei*. *Parasitology* **71:** 393–417.

De Greef, C., and Hamers, R. (1994) The serum resistance-associated (SRA) gene of *Trypanosoma brucei rhodesiense* encodes a variant surface glycoprotein-like protein. *Mol Biochem Parasitol* **68:** 277–284.

Engstler, M., Pfohl, T., Herminghaus, S., Boshart, M., Wiegertjes, G., Heddergott, N., and Overath, P. (2007) Hydrodynamic flow-mediated protein sorting on the cell surface of trypanosomes. *Cell* **131:** 505–515.

Grunfelder, C.G., Engstler, M., Weise, F., Schwarz, H., Stierhof, Y.D., Morgan, G.W., *et al.* (2003) Endocytosis of a glycosylphosphatidylinositol-anchored protein via clathrin-coated vesicles, sorting by default in endosomes, and exocytosis via RAB11-positive carriers. *Mol Biol Cell* **14:** 2029–2040.

Higgins, M.K., Tkachenko, O., Brown, A., Reed, J., Raper, J., and Carrington, M. (2013) Structure of the trypanosome haptoglobin-hemoglobin receptor and implications for nutrient uptake and innate immunity. *Proc Natl Acad Sci USA* **110:** 1905–1910.

Hirumi, H., and Hirumi, K. (1989) Continuous cultivation of *Trypanosoma brucei* blood stream forms in a medium containing a low concentration of serum protein without feeder cell layers. *J Parasitol* **75:** 985–989.

Landeira, D., Bart, J.M., Van Tyne, D., and Navarro, M. (2009) Cohesin regulates VSG monoallelic expression in trypanosomes. *J Cell Biol* **186:** 243–254.

Manna, P.T., Boehm, C., Leung, K.F., Natesan, S.K., and Field, M.C. (2014) Life and times: synthesis, trafficking, and evolution of VSG. *Trends Parasitol* **30:** 251–258.

Oli, M.W., Cotlin, L.F., Shiflett, A.M., and Hajduk, S.L. (2006) Serum resistance-associated protein blocks lysosomal targeting of trypanosome lytic factor in *Trypanosoma brucei*. *Eukaryot Cell* **5:** 132–139.

Pal, A., Hall, B.S., Jeffries, T.R., and Field, M.C. (2003) Rab5 and Rab11 mediate transferrin and anti-variant surface glycoprotein antibody recycling in *Trypanosoma brucei*. *Biochem J* **374:** 443–451.

Pays, E., Vanhollebeke, B., Uzureau, P., Lecordier, L., and Pérez-Morga, D. (2014) The molecular arms race between African trypanosomes and humans. *Nat Rev Microbiol* **12:** 575–584.

Penate, X., Lopez-Farfan, D., Landeira, D., Wentland, A., Vidal, I., and Navarro, M. (2009) RNA pol II subunit RPB7 is required for RNA pol I-mediated transcription in *Trypanosoma brucei*. *EMBO Rep* **10:** 252–257.

Perez-Morga, D., Vanhollebeke, B., Paturiaux-Hanocq, F., Nolan, D.P., Lins, L., Homble, F., *et al.* (2005) Apolipoprotein L-I promotes trypanosome lysis by forming pores in lysosomal membranes. *Science (New York, N.Y)* **309:** 469–472.

Stephens, N.A., and Hajduk, S.L. (2011) Endosomal localization of the serum resistance-associated protein in African trypanosomes confers human infectivity. *Eukaryot Cell* **10:** 1023–1033.

Sutterwala, S.S., Creswell, C.H., Sanyal, S., Menon, A.K., and Bangs, J.D. (2007) *De novo* sphingolipid synthesis is essential for viability, but not for transport of glycosylphosphatidylinositol-anchored proteins, in African trypanosomes. *Eukaryot Cell* **6:** 454–464.

Thomson, R., and Finkelstein, A. (2015) Human trypanolytic factor APOL1 forms pH-gated cation-selective channels in planar lipid bilayers: relevance to trypanosome lysis. *Proc Natl Acad Sci USA* **112:** 2894–2899.

Thomson, R., Molina-Portela, P., Mott, H., Carrington, M., and Raper, J. (2009) Hydrodynamic gene delivery of baboon trypanosome lytic factor eliminates both animal and human-infective African trypanosomes. *Proc Natl Acad Sci USA* **106:** 19509–19514.

Turner, C.M., McLellan, S., Lindergard, L.A., Bisoni, L., Tait, A., and MacLeod, A. (2004) Human infectivity trait in *Trypanosoma brucei*: stability, heritability and relationship to sra expression. *Parasitology* **129:** 445–454.

Uzureau, P., Uzureau, S., Lecordier, L., Fontaine, F., Tebabi, P., Homble, F., *et al.* (2013) Mechanism of *Trypanosoma brucei gambiense* resistance to human serum. *Nature* **501:** 430–434.

Vanhamme, L., Paturiaux-Hanocq, F., Poelvoorde, P., Nolan, D.P., Lins, L., Van Den Abbeele, J., *et al.* (2003) Apolipoprotein L-I is the trypanosome lytic factor of human serum. *Nature* **422:** 83–87.

Vanhollebeke, B., De Muylder, G., Nielsen, M.J., Pays, A., Tebabi, P., Dieu, M., *et al.* (2008) A haptoglobin-hemoglobin receptor conveys innate immunity to *Trypanosoma brucei* in humans. *Science (New York, N.Y)* **320:** 677–681.

Wirtz, E., Leal, S., Ochatt, C., and Cross, G.A. (1999) A tightly regulated inducible expression system for conditional gene knock-outs and dominant-negative genetics in *Trypanosoma brucei*. *Mol Biochem Parasitol* **99:** 89–101.

Xong, H.V., Vanhamme, L., Chamekh, M., Chimfwembe, C.E., Van Den Abbeele, J., Pays, A., *et al.* (1998) A VSG expression site-associated gene confers resistance to human serum in *Trypanosoma rhodesiense*. *Cell* **95:** 839–846.

Yeaman, C., Grindstaff, K.K., Wright, J.R., and Nelson, W.J. (2001) Sec6/8 complexes on trans-Golgi network and plasma membrane regulate late stages of exocytosis in mammalian cells. *J Cell Biol* **155:** 593–604.